

Surface morphology and internal layer stratigraphy in the downstream end of Kamb Ice Stream, West Antarctica

G.A. CATANIA,^{1*} H. CONWAY,¹ C.F. RAYMOND,¹ T.A. SCAMBOS²

¹*Department of Earth and Space Sciences, Box 351310, University of Washington, Seattle, Washington 98195-1310, USA
E-mail: gcatania@ig.utexas.edu*

²*National Snow and Ice Data Center, University of Colorado, Boulder, Colorado 80309-0449, USA*

ABSTRACT. Satellite images of Kamb Ice Stream (formerly Ice Stream C), West Antarctica, reveal several long, curved linear features (lineations) oriented sub-parallel to the ice-flow direction. We use ground-based radar to characterize the internal layer stratigraphy of these lineations and the terrains that they bound. Some lineations are relict ice-stream shear margins, identified by hyperbolic diffractors near the surface (interpreted to be buried crevasses) and highly disturbed internal layers at depth. Satellite images show another set of lineations outside the relict margins that wrap around the ends of the surrounding inter-ice-stream ridges. Internal layers beneath these lineations are downwarped strongly into a syncline shape. The internal stratigraphy of the terrain between these lineations and the relict margins is characterized by deep hyperbolic line diffractors. Our preferred hypothesis for the origin of this terrain is that it was floating sometime in the past; the deep hyperbolas are interpreted to be basal crevasses, and the strongly downwarped internal layers mark the position of a relict grounding line. Our study shows that lineations and intervening terrains have different internal layer characteristics implying different origins. Differentiation between these features is not possible using satellite images alone.

INTRODUCTION

Satellite images provide information about changes in ice-flow history through interpretation of the arrangement of visible flow features including crevasses, rifts, flow stripes and relict shear margins (Scambos and Bindschadler, 1993; Bindschadler and Vornberger, 1998; Fahnestock and others, 2000). Such features are associated with subtle topography (amplitudes of a few meters and wavelengths of several kilometers) not easily seen on the ground. Some flow features have a clear origin, such as crevasses and rifts, but the dynamic causes of the subtle topographic signatures associated with flow stripes and relict margins are often unclear. Supplementary information about the genesis and evolution of these features is necessary to characterize them and fully interpret their glacial origin.

We present results from ground-based, ice-penetrating radar profiles across satellite-detected lineations and terrains in the downstream end of Kamb Ice Stream (KIS; formerly Ice Stream C), West Antarctica, during the 2001/02 and 2002/03 field seasons (Fig. 1a). Kamb Ice Stream stagnated about 150 years ago (Retzlaff and Bentley, 1993); most of the lineations that are visible in satellite images of this region probably formed prior to stagnation. We distinguish three types of terrains and three types of lineations based on their surface morphology and their radar-detected internal stratigraphy. Figure 1a shows the location of acquired radar profiles and visible lineations (L1–L8). The north side of KIS includes an area called the ‘Duckfoot’, named for the splayed pattern of lineations that mark its surface (Jacobel and others, 2000). A similar area exists on the south side of KIS, and in the same spirit we call this the ‘Goosefoot’. These two regions consist of several different types of ice terrains,

each with distinct characteristics. Previous radar measurements obtained in the Duckfoot indicate that several of these features could be related to relict ice-stream margins (Jacobel and others, 2000). Our goal in this paper is to illustrate the differences in dynamic origin of the terrains and lineations in these two regions in order to aid in interpretation of the recent (~1000 year) ice-flow history.

RADAR AND SATELLITE DATA

BEDMAP data (Lythe and others, 2001) provide information regarding the bed topography and elevation above flotation for the downstream KIS area (Fig. 2). Bed topography is relatively high beneath the inter-ice-stream ridges and terrains surrounding KIS, and a ~300 m deep overdeepening exists in the mouth of KIS just upstream from the modern grounding line. Also, most of the ice in the mouth of Whillans Ice Stream (WIS) and KIS is within 50–100 m of flotation. The height above flotation is remarkably constant in the mouth of KIS but begins to increase toward the middle of the ice stream approaching the old UpC Camp (Fig. 2).

Several sources of satellite data are used to map lineations. Variations in brightness of a feature depend not only on its morphology but also on the satellite source and/or the illumination angle. We use data from two moderate-resolution (250–1100 m) satellites that provide information about the surface topography and albedo through variations in brightness: Advanced Very High Resolution Radiometer (AVHRR) imagery from US National Oceanic and Atmospheric Administration polar-orbiting weather satellites (Fig. 1c) and Moderate Resolution Imaging Spectroradiometer (MODIS) imagery from NASA (Fig. 1b). We also use high-resolution (25 m) synthetic aperture radar satellite (RADARSAT-1) data to derive a 125 m mosaic of our field site. Brightness in RADARSAT data comes from a combination of radar backscatter from both the surface and

* Present address: Institute for Geophysics, University of Texas, Austin, Texas 78759, USA

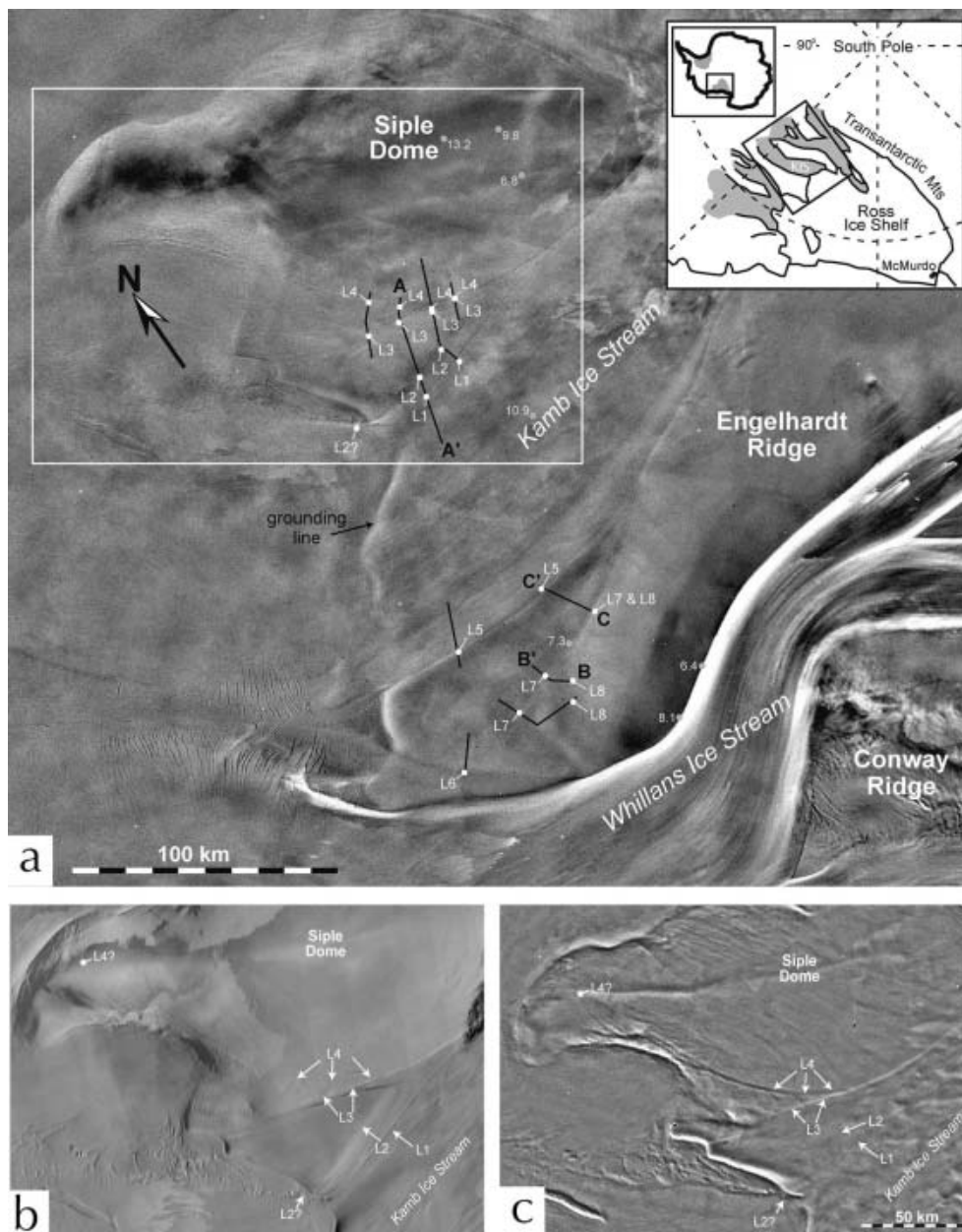


Fig. 1. (a) RADARSAT image of the Kamb and Whillans Ice Streams area. Flow direction is generally from right to left. Accumulation rates indicated with grey text are taken from Venteris and others (1998). Black lines show the location of nine radar profiles across lineations labeled L1–L8 (Table 1). Locations of lineations that have not been crossed with ice-penetrating radar data are labeled with a question mark. Radar profiles labeled A–C are shown in detail in Figures 3, 5 and 6. The white box outlines the area in (b) and (c). Inset shows our study area in West Antarctica. (b,c) MODIS (b) and AVHRR (c) images of the Duckfoot area and south flank of Siple Dome. Both images are at the same scale as (a).

subsurface: up to ~2 m on exposed ice and up to ~10 m on dry, cold firn (Rignot and others, 2001), which permits detection of crevasses that are thinly covered by accumulation. Active crevasse regions such as the north margin of WIS are bright in backscatter (Fig. 1a).

Two ground-based radar systems are used to study internal layer structure and bed characteristics. Of particular interest are changes in internal structure across the satellite-detected lineations. In most cases, these lineations mark boundaries between terrains with different origin. Continuous layers are classified as either smooth or distorted, a qualitative distinction that is based on changes in layer shape relative to changes in bed topography. We used a low-frequency (2–5 MHz) short-pulse radar system (described by Gades, 1998) to image deep internal layers (~100–1000 m) and the

bed. A pressure transducer and a geodetic-quality global positioning system (GPS) receiver were used to measure surface topography and elevations relative to the World Geodetic System 1984 (WGS84) ellipsoid; here the ellipsoid is ~45 m above present-day sea level. To map the near-surface stratigraphy we used a commercial high-frequency (50–200 MHz) radar system (RAMAC) with a corresponding resolution of 1–0.25 m. To improve the signal-to-noise ratio, we recorded radar waveforms that consist of several hundred stacked (averaged) waveforms acquired continuously over horizontal spacing that ranged from 1.5 to 5 m for high-frequency radar, and 10 to 25 m for low-frequency radar. As a result, steeply dipping internal layers may be aliased. Additional processing includes bandpass filtering, migration and conversion of two-way travel time to depth. We assume

the wave speed in ice is $168.5 \text{ m } \mu\text{s}^{-1}$ and account for higher wave speeds near the surface using depth–density measurements from the Siple Coast (Alley and Bentley, 1988) and the Looyenga mixing equation (Glen and Paren, 1975) to estimate depth variations of the dielectric constant.

CHARACTER AND ORIGIN OF LINEATIONS

1. Lineations associated with near-surface diffractors

Radar profiles across four of the lineations (L2, L3, L5 and L6) reveal near-surface diffractors and distorted, often discontinuous deep internal layers (Fig. 3a; Table 1). GPS measurements across these features show broad topographic troughs that are 10–50 m deep over 3–10 km. MODIS and AVHRR images of the Duckfoot (Fig. 1b and c) both show L2 and L3 as bright, narrow lines (which are likely to be due to these troughs) aligned, respectively, parallel and sub-parallel to the most recent flow direction of KIS as indicated by flow stripes in the main body of KIS. Radar data show that the near-surface diffractors are closer to the surface at L2 than L3. Because diffractors here are not distinct, we pick the depth of the deepest continuous internal layer: 30 m for L3 and 18 m for L2 (Fig. 3c and b, respectively). Two sets of near-surface diffractors are detected beneath the lineations on the Goosefoot: one at L5 (22 m below the surface) and another at L6 (17 m below the surface) (Fig. 1a).

We interpret these four lineations to be relict ice-stream shear margins now buried under >100 years of accumulation. The numerous near-surface diffractors associated with the lineations are interpreted to be buried crevasses that formed at the surface within a margin of an active ice stream. This interpretation is not new; Retzlaff and Bentley (1993) identified L5 as a relict margin of KIS, and Jacobel and others (2000) identified L3 as a relict margin. The deformed deep internal layer stratigraphy is consistent with conditions in an active ice stream where large cumulative strain is expected. Layer continuity here is lost due to some combination of high strain, causing steeply sloping layers, and signal loss from scattering within the near-surface diffractors. Deeper layers regain continuity about 10 km inside the ice-stream margin towards the middle of the ice stream. The discontinuous layers are probably related to the chaotic zones observed in active shear margins where strain rates are largest and crevassing does not conform to a particular pattern (Echelmeyer and Harrison, 1999).

Several characteristics of margins are apparent: the presence of near-surface point diffractors, deep discontinuous layers and the coincidence of these margins with broad topographic troughs, which are present across other active and relict ice-stream margins (Whillans and others, 1993; Gades and others, 2000; Conway and others, 2002; Catania and others, 2003). One possible explanation for trough formation is that focused strain heating in margins allows for localized melting (Jacobson and Raymond, 1998). Thorsteinsson and others (2003) show that ice advected across an ice-stream margin undergoes rapid changes in the stress pattern, such that the direction of maximum compression becomes horizontal. They argue that ice expands vertically as it traverses an ice-stream margin but indicate that recrystallization and crevasse formation may counter this. The troughs that we observe across ice-stream margins probably represent some combination of these processes.

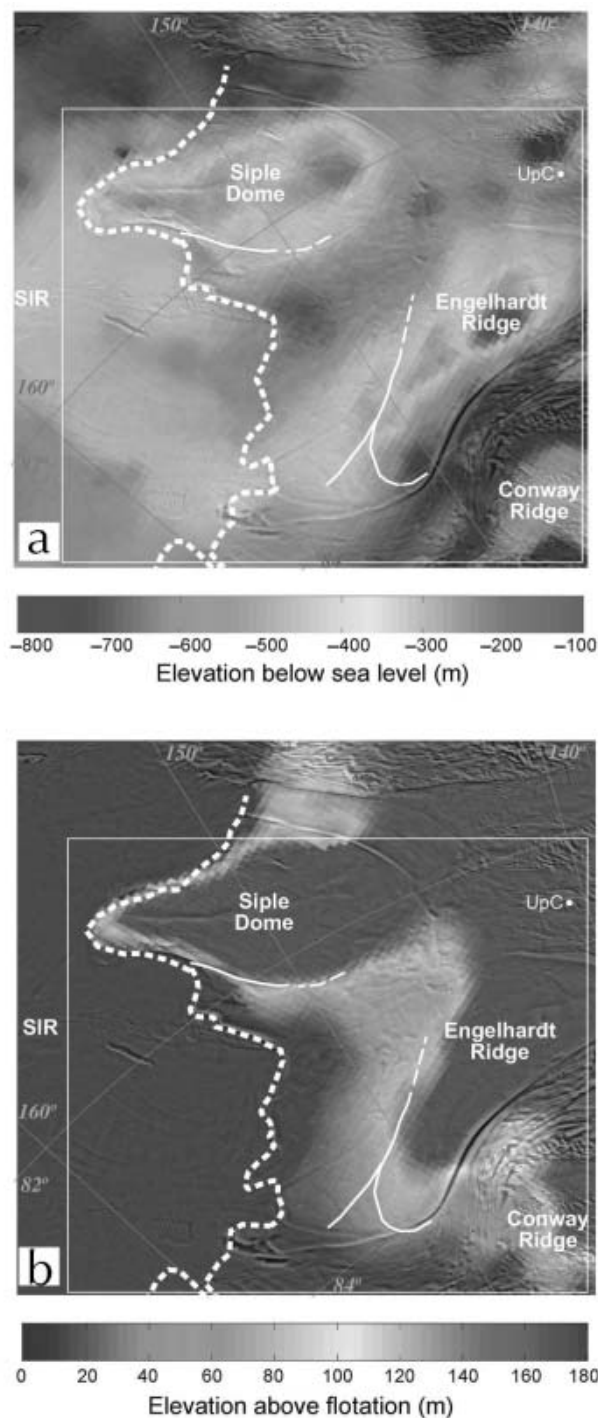


Fig. 2. (a) Bed elevation and (b) elevation above flotation for the KIS area based on BEDMAP data (Lythe and others, 2001). Data have a 5 km grid spacing, 1–5% vertical accuracy, and the vertical datum is corrected to the OSU91 geopotential model which deviates from mean sea level by an average of 1.5 m. The white box outlines the location of Figure 1a. Active margins and flowlines of Whillans and Bindschadler Ice Streams are visible in the underlying AVHRR image. The present-day grounding-line position is shown as a thick dashed white line. Positions of the syncline features (see text) are indicated by thin white solid lines. The dashed white line shows the possible extrapolation of syncline features across KIS. The greyscale bars saturate at values outside their limits.

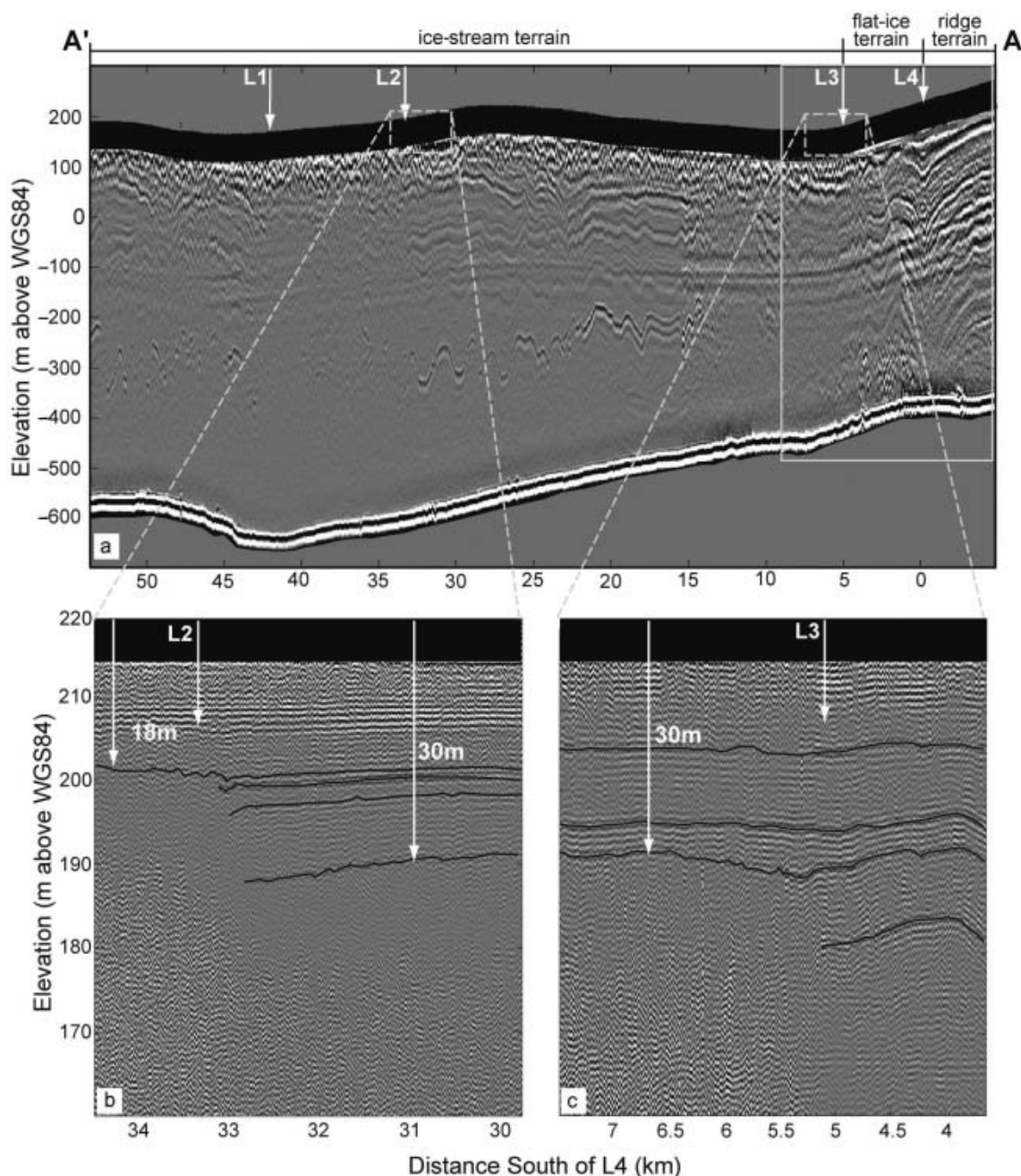


Fig. 3. (a) 2 MHz radar profile across L1–L4 along line A (Fig. 1a). The prominent return at approximately -100 m is a glitch in the transmitter. Data in the upper ~ 80 m (covered by a black band) are not resolved by the radar system. The solid grey line outlines the data shown in detail in Figure 4. (b) 100 MHz radar profile across L2. Arrows indicate the depth to the deepest continuous layer. (c) 100 MHz radar profile across L3. Prominent layers have been traced in each of the high-frequency radar profiles

2. Lineations associated with no change in internal layers

L1 is a distinct, narrow lineation parallel to the most recent flow direction of KIS (Table 1). It appears to originate at the junction between the southern edge of Siple Dome and the innermost margin of KIS and fades out about 20 km before the KIS grounding line. Our measurements show that L1 is a low-amplitude (~ 2 m), long-wavelength (~ 2 km) undulation in surface topography, which appears as an alternating light and dark pattern in Figure 1a and b. Both high- and low-frequency radar profiles across L1 show deep disturbed layers and near-surface diffractors beneath the surface undulation.

The depth to near-surface diffractors does not change across L1, and so we do not think this is a relict margin of

KIS, as hypothesized by Jacobel and others (2000). Instead we believe it is a relict flow stripe that originated from within an active shear margin. Merry and Whillans (1993, figs 5 and 7) show several examples where flow stripes originate from margins of active ice streams, and Gudmundsson and others (1998) show flow stripes with similar geometry to that of L1 in satellite images.

3. Lineations associated with syncline layers

Three of the eight lineations examined (L4, L7 and L8) are associated with shallow topographic troughs (~ 1 – 3 m deep) that span only a few kilometers (Table 1). On the surface, such small-scale topographic changes are not easily discernible but they are visible in satellite images, especially

Table 1. Main characteristics of features labeled in Figure 1 and described in text

Lineation	Origin	Layer structure	Alignment	Topography
L1	Flow stripe	No layer change	with flow	1–2 m deep undulation
L2	Relict margin	Buried crevasses, deep distorted layers	with flow	10–50 m deep trough
L3	Relict margin	Buried crevasses, deep distorted layers	with flow	10–50 m deep trough
L4	Grounding line	Layer syncline, deep diffractors	around ridge	1–3 m deep trough
L5	Relict margin	Buried crevasses, deep distorted layers	with flow	10–50 m deep trough
L6	Relict margin	Buried crevasses, deep distorted layers	with flow	10–50 m deep trough
L7	Grounding line	Layer syncline, deep diffractors	around ridge	1–3 m deep trough
L8	Grounding line	Layer syncline, deep diffractors	with flow	1–3 m deep trough

when taken at low Sun angles. These lineations are found at the boundaries between inter-ice-stream ridges and the flat-ice terrains in the mouth of KIS. In the Duckfoot, L4 wraps alongside the southern edge of Siple Dome, diverging away from the paleo-flow direction of KIS towards the grounding line (Fig. 1c). On the south side of KIS in the Goosefoot, L7 also wraps around the western end of Engelhardt Ridge away from the paleo-flow direction of KIS (Fig. 1a). L7 branches away from the edge of the ridge where it merges with L8 and cuts across the Goosefoot towards the grounding line (Fig. 1a).

Internal layers beneath these troughs are warped downwards as much as 200 m, forming a syncline that is unrelated to bed topography (Figs 4–6). The fold amplitude of these synclines increases with depth, and the deepest layers are truncated at the bed. The fold axis of the syncline in the Duckfoot is tilted away from Siple Dome such that the trough of the uppermost isochrone is offset horizontally by ~150 m from that of the deepest isochrone (Fig. 4). Assuming that the mechanism causing the downwarp maintained a consistent spatial pattern over time, this offset is probably caused by flow off Siple Dome after the syncline formed. If the present-day surface velocities (0.9 m a^{-1} ; Jacobel and others, 2000) have been constant over the past few hundred years, the processes forming the syncline would have stopped about 170 years ago. Synclines in the Goosefoot (L7 and L8) have vertical fold axes (Fig. 6), implying that the processes causing these synclines may still be active or only recently ceased, although slope-driven flow across L7 might be too low to cause a noticeable tilt in the syncline axis. The most distinct characteristic of L7 is that it marks the location where the depth of deep diffractors changes (Fig. 5). We note that the B-line profile across L7 does not show downwarped layers (Fig. 5), but the other radar profile across L7 (not shown) does.

Several mechanisms could cause downwarping of internal layers. For example, Vaughan and others (1999) attribute near-surface downwarped internal layers across the boundary between an inter-ice-stream ridge and a possible relict ice stream to a localized high accumulation. Their data show that the amplitude of the layer syncline increases with depth in the upper 100 m of ice and they attribute this to a 33% increase in accumulation at the slope break between

the ridge and the area of flat ice adjacent to it. Several layers across the upper 30 m (~350 years) of the Goosefoot and Duckfoot syncline-layer boundaries do not show changes in layer thickness that might suggest an accumulation anomaly here for at least the past few hundred years.

Localized basal melting can also downwarp internal layers over a narrow region. Basal melting can occur through several processes including melt beneath an ice shelf at the grounding line (Gill, 1973; Smith, 1996; Rignot and Jacobs, 2002), melt from a localized high geothermal flux (Fahnestock and others, 2001) and melting due to strain heating within shear margins (Jacobson and Raymond, 1998). We do not think the observed stratigraphy is consistent with that of typical relict ice-stream margins, for several reasons: (1) high-frequency radar data across L4, L7 and L8 do not show near-surface point diffractors, while relict ice streams (e.g. 'Siple Ice Stream') as old as 420 ± 60 years (personal communication from B. Smith, 2000) still show evidence of near-surface point diffractors; (2) both L4 and L8 wrap around the edges of inter-ice-stream ridges away from the paleo-flow direction of KIS; (3) deep layers are preserved across these features, indicating that strain rates were not as high as those observed in present-day margins; (4) there is no evidence of flow stripes (indicative of sliding) on the surface in the areas adjacent to the syncline lineations; and (5) radar profiles across known relict and active shear margins do not show localized downwarping to this degree. Rather, the pattern of deeper layers across ice-stream margins appears to be disorganized (Gades and others, 2000; Catania and others, 2003).

Variable geothermal heat sources could potentially produce the observed melt signature. The syncline-layer boundaries appear to be associated with the edges of the inter-ice-stream ridges which may represent geologic as well as topographic boundaries. Geomagnetic data are not available for this region to determine whether local anomalous heat sources are a possibility (Sweeney and others, 1999). Because of this, we are not able to rule out the possibility that these syncline-layer boundaries result from a geothermal anomaly. However, this mechanism gives no explanation for the deep line diffractors seen in adjacent terrains. It is possible that the diffractors and the synclines are unrelated, but we search for a hypothesis that can simply explain all observations.

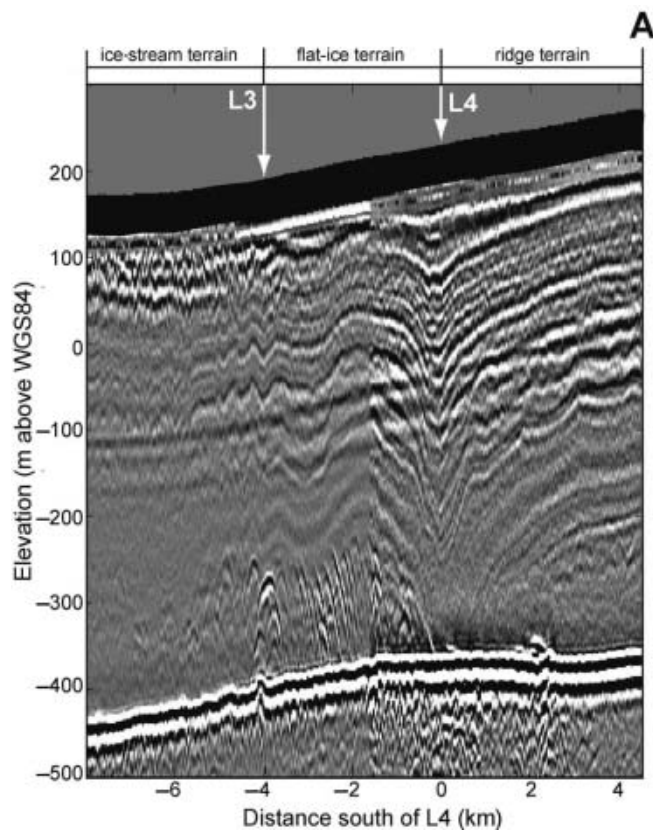


Fig. 4. 2 MHz radar profile along a section of line A (as shown in the box outlined in Fig. 3a) crossing L4 and the northernmost KIS margin (L3). The prominent return at approximately -100 m elevation is a glitch in the transmitter. Data in the upper ~ 80 m (covered by a black band) are not resolved by the radar system.

Our preferred hypothesis is that the melting occurred near a grounding line when the region was once floating. Grounding-line melt occurs at the back of a sub-ice-shelf cavity through the circulation of high-salinity shelf-water (HSSW) which is produced when salt is rejected during the formation of sea ice (MacAyeal, 1985). HSSW is delivered along the seabed to the grounding line and can remain up to 0.5°C warmer than the in situ freezing point of water beneath the ice-shelf base (Gill, 1973). HSSW can induce basal melting, but strong stratification often prevents its contact with the ice-shelf base. MacAyeal (1984) shows that large tidal currents, developed in areas with a small water column thickness (such as at grounding lines), can stir the water column and promote localized basal melting. The pattern of grounding-line melt is not clear; some modelling predicts that melt would be spread over wide (~ 100 km) areas downstream of the grounding line (Jenkins and Doake, 1991), although limited observational evidence indicates that it could be more focused (<10 km) near the grounding line (Smith, 1996).

CHARACTER AND ORIGIN OF TERRAINS

1. Ridge terrain

Inter-ice-stream ridges (e.g. Siple Dome and Engelhardt Ridge in Fig. 7) rise several hundred meters above the surrounding ice streams, but have a smooth surface topography over scales of hundreds of meters (Fig. 1). Surface velocities are slow, $<8\text{ m a}^{-1}$ (Whillans and Van der

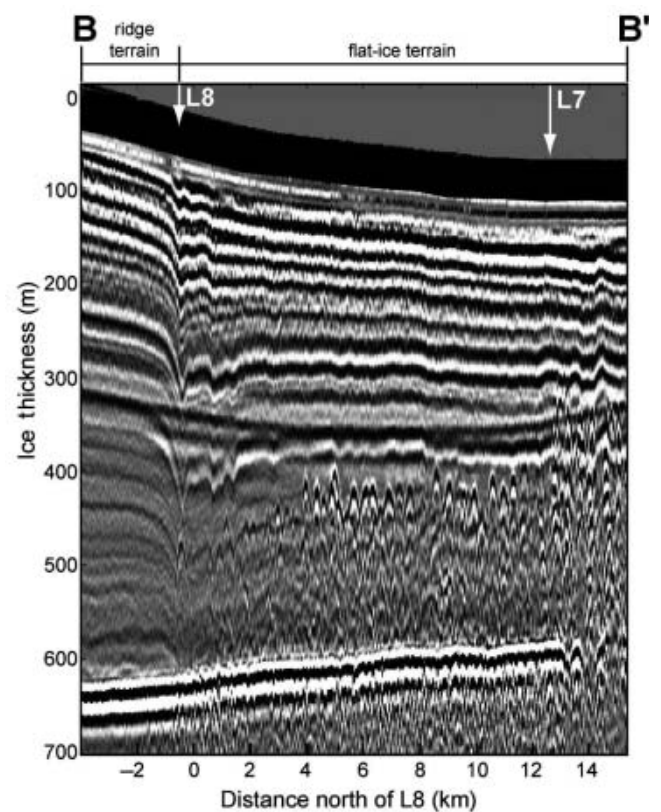


Fig. 5. 2 MHz data along line B in the Goosefoot crossing L7 and L8 (Fig. 1a). Note the prominent return at ~ 300 m depth is a glitch in the transmitter. Data in the upper ~ 80 m (covered by a black band) are not resolved by the radar system.

Veen, 1993), and radar profiles generally reveal continuous internal layers with undulations that appear as smoothed versions of the bed topography (Nereson and others, 2000).

2. Ice-stream terrain

Rose (1979) deduced that Ice Stream C (here called KIS) had stagnated, based on a lack of visible surface crevasses compared to other ice streams. Satellite images confirm this observation but also show that the surface topography of KIS is complex and more undulating than the surrounding inter-ice-stream ridges and flat-ice terrains (Fig. 1). Typical slopes of ice-stream terrain are $\sim 10^{-3}$ and although KIS is now slow-moving ($0.1\text{--}10\text{ m a}^{-1}$), numerous flow stripes still visible on the surface and buried marginal crevasses provide evidence of fast flow in the past. Typical internal structure within ice-stream terrain includes near-surface diffractors and deeper layers that are often continuous but highly distorted due to the large cumulative strain. Relict and active ice-stream terrains are indicated in Figure 7.

3. Flat-ice terrain

Flat-ice terrain is a distinctive, previously undefined, terrain type that lies between the inter-ice-stream ridges and the main body of relict KIS. Surface slope (10^{-4}) and velocities ($<0.3\text{ m a}^{-1}$) are small (Jacobel and others, 2000) and the surface topography across these regions is smoother than ice-stream terrain but rougher than ridge terrain (Fig. 1).

Radar-detected stratigraphy across these areas shows layers that are continuous and lightly disturbed in the upper

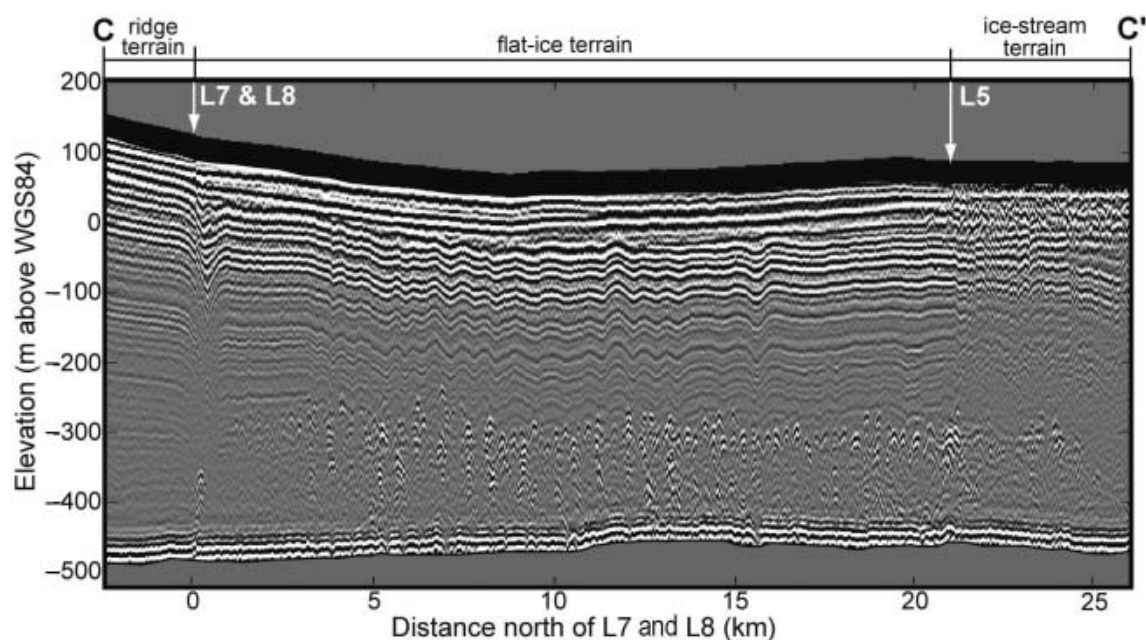


Fig. 6. 5 MHz radar profile along line C in the Goosefoot crossing L5, L7 and L8. Data in the upper ~80 m (covered by a black band) are not resolved by the radar system.

half of the ice, but discontinuous, with numerous diffractors, in the lower half of the ice (Fig. 6). These diffractors extend throughout the flat-ice terrains from their boundary with the inter-ice-stream ridges at the location of L4 and L8 to several kilometers (up to 10 km in Goosefoot) into the relict shear margins of KIS. The diffractors occur in distinct sets with uniform heights. In the Duckfoot there is one set ~150 m above the bed (Fig. 4), while in the Goosefoot there are two sets of diffractors: one ~200 m above the bed and another ~250 m above the bed (Figs 6 and 5). The transition between the two sets of diffractors in the Goosefoot occurs at L7.

Although the pattern of layer distortion above these diffractors appears to be random in the Duckfoot, it is partly organized in the Goosefoot. Figure 6 shows that the upper layers in the Goosefoot undulate with a wavelength of ~1 km; peaks in the layers roughly align with the tops of diffractors below them. Other profiles in the Goosefoot (Fig. 5) show flat layers overlying diffractors, implying that this organized pattern may not be widespread.

Grid and star patterns of radar data from across deep diffractors in the Goosefoot and Duckfoot reveal more information about diffractor geometry and orientation. Radar profiles across diffractors in directions perpendicular to L4 and L8 show diffraction hyperbolas, and migration of radar data along the C-line profile (Fig. 6) reduces these hyperbolas to point sources. In contrast, radar profiles in directions parallel to L4 and L8 show a line diffractor at the same depth as the top of the hyperbolas. This pattern is indicative of a source of contrasting permittivity along a line oriented parallel to L4 and L8.

We are not certain of the origin of the deep diffractors in these terrains. We rule out the possibility that they are buried surface crevasses because at such depths crevasses would be closed, reducing the permittivity contrast necessary to produce a diffractor. Clarke and others (2000) found similar deep diffractors in the small inter-ice-stream ridge between the two limbs of Whillans Ice Stream (the Unicorn). They proposed several possible causes for the diffractors including

the presence of basal crevasses, englacial morainal debris and a residual zone of temperate ice produced within the high-strain-rate environment of an active shear margin. Unlike the Clarke diffractors, diffractors in these flat-ice terrains occur up to 20 km away from relict shear margins and so we discount that they originated as temperate ice zones within shear margins.

Debris-rich ice can be accreted to the base of the ice column as seen beneath parts of KIS (personal communication from H. Engelhardt, 2001). Kamb (2001) calculated freeze-on at the UpC camp of 0.0045 m a^{-1} from borehole

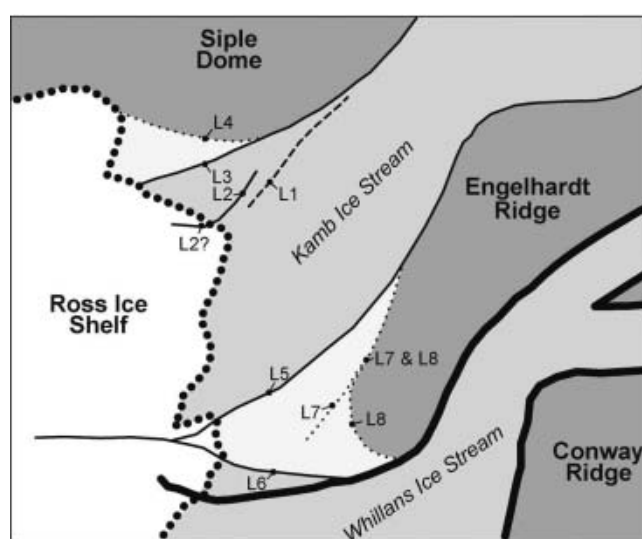


Fig. 7. Lineations and terrains of lower KIS and WIS mapped from Figure 1. Flat-ice terrains are light grey, inter-ice stream ridges are dark grey, and ice-stream terrains are medium-grey. The modern grounding line is a thick dotted line, and the hypothesized relict grounding lines are thin dotted lines. Active ice-stream margins are shown as thick black lines while relict margins are thin black lines.

data, and rates of up to 0.1 m a^{-1} have been reported beneath Matanuska Glacier, Alaska, USA (Lawson and others, 1998). Even using this high rate, accretion of 250–300 m of basal ice (the height of the point diffractors above the bed) would take at least 2500 years. Although we do not rule out basal freeze-on, we suspect that other processes dominate.

Similar diffractor features have been detected in airborne-radar profiles over ice shelves (Jezek and others, 1979; Jezek and Bentley, 1983). These are usually interpreted to be basal crevasses formed in floating ice. Tops of basal crevasses are likely to produce a strong reflection, especially if pockets of brine are trapped within them prior to crevasse closure. For a free-floating ice shelf of thickness H , Weertman (1980) calculated that a single bottom crevasse could penetrate up to $\pi H/4$. In the case of multiple basal crevasses, penetration height is expected to be lower ($\sim H/2$) because the stress causing crevasse formation is spread over multiple crevasse tips (Van der Veen, 1998). The remarkably constant height of these diffractors above the bed across large regions of these terrains might suggest that large areas were susceptible to a similar stress environment. The height of basal crevasses can be increased through tidal flexing of the ice shelf. Diffractor orientation supports the idea that, if these features are basal crevasses, they formed from increased tensile stress as ice flowed from the ridges into floating and/or faster-moving ice.

If these diffractors were caused by basal crevasses, an implication is that these terrains were once floating, which is consistent with the hypothesis that the syncline features described above formed through basal melting at relict grounding lines (marking the outermost boundary of these terrains). However, the ice in these terrains is presently grounded (Fig. 2b); in order for these regions to be floating they would have to have been 50–100 m thinner or sea level must have been much higher than at present (Fig. 2).

SYNOPSIS

Although satellite images clearly illuminate the three types of lineations (Table 1), their different origins are difficult to distinguish from the satellite data alone. Relict margins are associated with the greatest topographic relief (10–50 m vertically over 3–10 km) while topographic changes across syncline lineations and flow stripes are much smaller (1–2 m over 1–2 km). Supplementary ground-based radar measurements are needed to differentiate the characteristics and possible origins of these features. This is crucial to an accurate interpretation of ice-flow history.

Jacobel and others (2000) were the first to complete ground-based radar surveys in the Duckfoot region. They acquired 5 MHz data along profile C (Fig. 1) and showed that the northern margin of KIS had shifted inward prior to complete shut-down of the ice stream. However, without the advantage of high-frequency radar to image the near-surface structure, they identified L1 as the most recent margin of KIS. Our data show that the depth to buried crevasses does not change from L2 to L1 and into the main body of KIS for several kilometers, indicating that L2 is the most recent margin and that L1 is probably a flow stripes originating from within this margin.

Radar profiles discussed by Jacobel and others (2000) cross L3 and L4 where they are nearly coincident (Fig. 1), which hampers interpretation of these two lineations. Our profiles farther downstream show clearly that the internal

stratigraphy of L4 is quite distinct from L3, and it is not a relict ice-stream shear margin.

Our radar investigations reveal three different types of terrains in the mouth of KIS, including a newly defined flat-ice terrain (Fig. 7). These terrains, located between inter-ice-stream ridges and relict ice streams, are characterized by numerous mid-depth line diffractors. The simplest explanation is that these diffractors are caused by bottom crevasses, and we suggest that these terrains were once part of a relict ice shelf that occupied the mouth of KIS. Consistent with this hypothesis are internal layer synclines that mark the boundary of the flat-ice terrains with the inter-ice-stream ridges. These synclines may have been created through focused basal melting, which can occur at grounding lines (Gill, 1973; Smith, 1996; Rignot and Jacobs, 2002). Further, the surface lineations wrap around the ends of inter-ice-stream ridges, suggestive of a relict grounding line rather than relict flow features of KIS. This interpretation implies retreat and readvance of the grounding line by ~ 100 km. Our hypothesis suggests that the large-scale pattern of grounding-line retreat over the past 7500 years (e.g. Conway and others, 1999) may have been periodically interrupted by readvance some time during the past millennium.

ACKNOWLEDGEMENTS

We thank A. Gades, M. Conway and Raytheon Polar Services support staff for valuable contributions in the field. Imagery for this work was provided through the Antarctic Glaciological Data Center at NSIDC. We are grateful to J. Kohler and an anonymous reviewer whose comments led to significant improvements to the paper, and to H. Rott who served as scientific editor. This work was supported by the National Science Foundation (US grant OPP-9909518).

REFERENCES

- Alley, R.B. and C.R. Bentley. 1988. Ice-core analysis on the Siple Coast of West Antarctica. *Ann. Glaciol.*, **11**, 1–7.
- Bindschadler, R. and P. Vornberger. 1998. Changes in the West Antarctic ice sheet since 1963 from declassified satellite photography. *Science*, **279**(5351), 689–692.
- Catania, G.A., H.B. Conway, A.M. Gades, C.F. Raymond and H. Engelhardt. 2003. Bed reflectivity beneath inactive ice streams in West Antarctica. *Ann. Glaciol.*, **36**, 287–291.
- Clarke, T.S., C. Liu, N.E. Lord and C.R. Bentley. 2000. Evidence for a recently abandoned shear margin adjacent to Ice Stream B2, Antarctica, from ice-penetrating radar measurements. *J. Geophys. Res.*, **105**(B6), 13,409–13,422.
- Conway, H., B.L. Hall, G.H. Denton, A.M. Gades and E.D. Waddington. 1999. Past and future grounding-line retreat of the West Antarctic ice sheet. *Science*, **286**(5438), 280–283.
- Conway, H., G. Catania, C. Raymond, T. Scambos, H. Engelhardt and A. Gades. 2002. Switch of flow direction in an Antarctic ice stream. *Nature*, **419**(6906), 465–467.
- Echelmeyer, K.A. and W.D. Harrison. 1999. Ongoing margin migration of Ice Stream B, Antarctica. *J. Glaciol.*, **45**(150), 361–369.
- Fahnestock, M.A., T.A. Scambos, R.A. Bindschadler and G. Kvaran. 2000. A millennium of variable ice flow recorded by the Ross Ice Shelf, Antarctica. *J. Glaciol.*, **46**(155), 652–664.
- Fahnestock, M., W. Abdalati, I. Joughin, J. Brozena and P. Gogineni. 2001. High geothermal heat flow, basal melt, and the origin of rapid ice flow in central Greenland. *Science*, **294**(5550), 2338–2342.

- Gades, A.M. 1998. Spatial and temporal variations of basal conditions beneath glaciers and ice sheets inferred from radio echo soundings. (PhD thesis, University of Washington.)
- Gades, A.M., C.F. Raymond, H. Conway and R.W. Jacobel. 2000. Bed properties of Siple Dome and adjacent ice streams, West Antarctica, inferred from radio-echo sounding measurements. *J. Glaciol.*, **46**(152), 88–94.
- Gill, A.E. 1973. Circulation and bottom water production in the Weddell Sea. *Deep-Sea Res.*, **20**(2), 111–140.
- Glen, J.W. and J.G. Paren. 1975. The electrical properties of snow and ice. *J. Glaciol.*, **15**(73), 15–38.
- Gudmundsson, G.H., C.F. Raymond and R. Bindschadler. 1998. The origin and longevity of flow stripes on Antarctic ice streams. *Ann. Glaciol.*, **27**, 145–152.
- Jacobel, R.W., T.A. Scambos, N.A. Nereson and C.F. Raymond. 2000. Changes in the margin of Ice Stream C, Antarctica. *J. Glaciol.*, **46**(152), 102–110.
- Jacobson, H.P. and C.F. Raymond. 1998. Thermal effects on the location of ice stream margins. *J. Geophys. Res.*, **103**(B6), 12,111–12,122.
- Jenkins, A. and C.S.M. Doake. 1991. Ice–ocean interaction on Ronne Ice Shelf, Antarctica. *J. Geophys. Res.*, **96**(C1), 791–813.
- Jezeq, K.C. and C.R. Bentley. 1983. Field studies of bottom crevasses in the Ross Ice Shelf, Antarctica. *J. Glaciol.*, **29**(101), 118–126.
- Jezeq, K.C., C.R. Bentley and J.W. Clough. 1979. Electromagnetic sounding of bottom crevasses on the Ross Ice Shelf, Antarctica. *J. Glaciol.*, **24**(90), 321–330.
- Kamb, B. 2001. Basal zone of the West Antarctic ice streams and its role in lubrication of their rapid motion. In Alley, R.B. and R.A. Bindschadler, eds. *The West Antarctic ice sheet: behavior and environment*. Washington, DC, American Geophysical Union, 157–199. (Antarctic Research Series, 77.)
- Lawson, D.E., J.C. Strasser, E.B. Evenson, R.B. Alley, G.J. Larson and S.A. Arcone. 1998. Glaciohydraulic supercooling: a freeze-on mechanism to create stratified, debris-rich basal ice. I. Field evidence. *J. Glaciol.*, **44**(148), 547–562.
- Lythe, M.B., D.G. Vaughan and BEDMAP consortium. 2001. BEDMAP: a new ice thickness and subglacial topographic model of Antarctica. *J. Geophys. Res.*, **106**(B6), 11,335–11,351.
- MacAyeal, D.R. 1984. Thermohaline circulation below the Ross Ice Shelf: a consequence of tidally induced vertical mixing and basal melting. *J. Geophys. Res.*, **89**(C1), 597–606.
- MacAyeal, D.R. 1985. Tidal rectification below the Ross Ice Shelf. In Jacobs, S.S., ed. *Oceanology of the Antarctic continental shelf*. Washington, DC, American Geophysical Union, 109–132. (Antarctic Research Series, 43.)
- Merry, C.J. and I.M. Whillans. 1993. Ice-flow features on Ice Stream B, Antarctica, revealed by SPOT HRV imagery. *J. Glaciol.*, **39**(133), 515–527.
- Nereson, N.A., C.F. Raymond, R.W. Jacobel and E.D. Waddington. 2000. The accumulation pattern across Siple Dome, West Antarctica, inferred from radar-detected internal layers. *J. Glaciol.*, **46**(152), 75–87.
- Retzlaff, R. and C.R. Bentley. 1993. Timing of stagnation of Ice Stream C, West Antarctica, from short-pulse radar studies of buried surface crevasses. *J. Glaciol.*, **39**(133), 553–561.
- Rignot, E. and S.S. Jacobs. 2002. Rapid bottom melting widespread near Antarctic ice sheet grounding lines. *Science*, **296**(5575), 2020–2023.
- Rignot, E., K. Echelmeyer and W. Krabill. 2001. Penetration depth of interferometric synthetic-aperture radar signals in snow and ice. *Geophys. Res. Lett.*, **28**(18), 3501–3504.
- Rose, K.E. 1979. Characteristics of ice flow in Marie Byrd Land, Antarctica. *J. Glaciol.*, **24**(90), 63–75.
- Scambos, T.A. and R. Bindschadler. 1993. Complex ice stream flow revealed by sequential satellite imagery. *Ann. Glaciol.*, **17**, 177–182.
- Smith, A.M. 1996. Ice shelf basal melting at the grounding line, measured from seismic observations. *J. Geophys. Res.*, **101**(C10), 22,749–22,755.
- Sweeney, R., C.A. Finn, D.D. Blankenship, R.E. Bell and J.C. Behrendt. 1999. Central West Antarctic aeromagnetic data: a web site for distribution of data and maps. *US Geol. Surv. Open File Rep.* 99-420.
- Thorsteinsson, T., E.D. Waddington and R.C. Fletcher. 2003. Spatial and temporal scales of anisotropic effects in ice-sheet flow. *Ann. Glaciol.*, **37**, 40–48.
- Van der Veen, C.J. 1998. Fracture mechanics approach to penetration of bottom crevasses on glaciers. *Cold Reg. Sci. Technol.*, **27**(3), 213–223.
- Vaughan, D.G., H.F.J. Corr, C.S.M. Doake and E.D. Waddington. 1999. Distortion of isochronous layers in ice revealed by ground-penetrating radar. *Nature*, **398**(6725), 323–326.
- Venteris, E. and I. Whillans. 1998. Variability of accumulation rate in the catchments of Ice Streams B, C, D and E, Antarctica. *Ann. Glaciol.*, **27**, 227–230.
- Weertman, J. 1980. Bottom crevasses. *J. Glaciol.*, **25**(91), 185–188.
- Whillans, I.M. and C.J. Van der Veen. 1993. New and improved determinations of velocity of Ice Streams B and C, West Antarctica. *J. Glaciol.*, **39**(133), 483–490.
- Whillans, I.M., M. Jackson and Y.H. Tseng. 1993. Velocity pattern in a transect across Ice Stream B, Antarctica. *J. Glaciol.*, **39**(133), 562–572.

MS received 1 December 2004 and accepted in revised form 10 June 2005